Organic fouling in forward osmosis (FO): Membrane flux behavior and foulant quantification

Shengji Xia [*], Lijuan Yao, Ruilin Yang and Yumin Zhou

State Key laboratory of Pollution Control and Resources Reuse, Tongji University, Shanghai, 200092, China

Abstract. Forward osmosis (FO) is an emerging membrane technology with potential applications in desalination and wastewater reclamation. The osmotic pressure gradient across the FO membrane is used to generate water flux. In this study, flux performance and foulant deposition on the FO membrane were systematically investigated with a co-current cross-flow membrane system. Sodium alginate (SA), bovine serum albumin (BSA) and tannic acid (TA) were used as model foulants. Organics adsorbed on the membrane were peeled off via oscillation and characterized by Fourier transform infrared (FTIR) spectroscopy and scanning electron microscopy (SEM). When an initial flux of 8.42 L/m^{2}h was applied, both flux reduction and foulant deposition were slight for the feed solution containing BSA and TA. In comparison, flux reduction and foulant deposition were much more severe for the feed solution containing SA, as a distinct SA cake-layer was formed on the membrane surface and played a crucial role in membrane fouling. In addition, as the initial SA concentration increased in FS, the thickness of the cake-layer increased remarkably, and the membrane fouling became more severe.

Keywords: forward osmosis; membrane fouling; permeate flux; adsorption

1. Introduction

Membrane-based separation processes have gained increasing interest over the last three decades and have become one of the most promising technologies in the 21st century (Guo *et al.* 2012). Membrane-based filtration is widely used in seawater desalination (Shaffer *et al.* 2012) and wastewater reuse (Bennett 2005). Currently, nanofiltration (NF) is one of the most effective and robust technologies among the membrane-based technologies for the separation of from water. However, increasing attention has been paid to energy consumption due to the severe energy crisis. Reverse osmosis (RO) processes require high pressure, thus making them relatively energy intensive. In addition, the inevitable fouling in RO increases the cost of energy consumption (Mylon *et al.* 2004).

Forward osmosis (FO) is an osmotic pressure-driven membrane separation process in which water flows across a semi-permeable membrane from a low-osmotic-pressure feed solution (FS) to a high-osmotic-pressure draw solution (DS) (Cath *et al.* 2006, Zhao *et al.* 2012). Compared with the traditional pressure-driven membrane processes, such as ultrafiltration, nanofiltration and

---

∗Corresponding author, Ph.D., E-mail: xiashengji@tongji.edu.cn

reverse osmosis, FO provides the advantage of lower energy consumption. In recent years, FO was found to have application potential in various fields, such as seawater desalination (McCutcheon *et al.*), wastewater treatment (McCutcheon *et al.* 2007, Cornelissen *et al.* 2008) and power generation via the pressure-retarded osmosis process (Chou *et al.* 2012, She *et al.* 2012).

Fouling in membrane separation process influences the membrane performance significantly (Lay *et al.* 2011, Tang *et al.* 2011). One potential advantage of FO is that it operates under the osmotic pressure difference across the semi-permeable FO membrane, which may result in reduced fouling compared with pressure-driven membrane processes due to minimal cake layer compaction. The fouling behaviour of FO and RO were compared in a wastewater treatment application (Holloway *et al.* 2007). A slower flux decline rate was observed in FO than that in RO. However, the fouling in the FO process still cannot be ignored. A number of previous FO studies using a variety of foulants, such as Aldrich humic acid, sodium alginate and bovine serum albumin, have demonstrated a decrease in the water permeate fluxes (Lay *et al.* 2011, Lee *et al.* 2010, Tang *et al.* 2010, Zhang *et al.* 2012). In addition, the fouling of an FO membrane is also affected by chemical and hydrodynamic factors, including temperature, calcium binding, permeation drag and shear forces, due to the development of a fouling layer on the membrane surface (Mi and Elimelech 2008, Phuntsho *et al.* 2012).

This paper aimed to evaluate the influence of organic fouling on the performance of a FO separation process. Sodium alginate, bovine serum albumin and tannic acid were selected as model foulants. SA and BSA were used as model organic foulants to represent common polysaccharides and proteins respectively. These organic macromolecules have been reported to be the major components of organic fouling during membrane filtration of surface water, seawater, and wastewater effluent (Grant *et al.* 1973, Ma *et al.* 2001). TA, a soluble refractory polyphenolic compound, is frequently found in most surface water, making tannic acid an attractive surrogate for the medium molecular weight materials due to its availability and controlled composition as well as its molecular weight distribution, which is similar to the range of major DOMs in raw surface water (Dalton *et al.* 2005, Lin *et al.* 2007). Although numerous studies had reported the influence of membrane fouling in general FO processes (Lee *et al.* 2010, She *et al.* 2003, Linares *et al.* 2012), only a few studies briefly conveyed the quantity of organics adsorbed onto the membrane and the relationship between the quantity of adsorbed organics and the decline of water permeate flux (Gu *et al.* 2013). In this study, in addition to determining the water permeate flux and the adsorption of organic foulants, the morphology and the structure of the FO membranes were characterized by Fourier transform infrared (FTIR) spectroscopy and scanning electron microscopy (SEM); the morphology characterization and adsorption quantification were combined to evaluate the influence of organic fouling on the performance of the forward osmosis process.

2. Materials and method

2.1 FO membranes

The forward osmosis membrane used in this study was a CTA-NW FO membrane provided by Hydration Technology Innovations, Inc. (Albany, OR). The membrane has an asymmetric structure with a filtration layer of cellulose acetate (CTA) and a supporting layer of a non-woven backing consisting of polyester fibres individually coated with polyethylene, according to Wei *et al.* (2011); the membrane is characterized by a thickness of 144 ± 24 μm, a porosity of $50 \pm 2\%$, an

s value of 1.38 ± 0.26 mm, and a contact angle of 74 ± 3°. The membrane was pre-treated before the experiments via soaking in deionized water for several hours to remove the glycerine from the membrane surface.

2.2 Chemicals

All of the reagents and chemicals used in the experiment were of analytical grade. Ultrapure water with a conductivity of 18.2 MΩ.cm (Millipore) was used to prepare all of the standard solutions. Sodium alginate, bovine serum albumin, tannic acid and sodium chloride purchased from Sinopharm Chemical Reagent Co. (China, Ltd) were used to prepare the feed solutions with the ultrapure water.

2.3 Bench-scale FO experiment

The schematic diagram of the FO filtration system is depicted in Fig. 1. A flat-sheet bench-scale FO membrane was installed in a membrane cell with equally structured channels on each side. The effective area of the FO membrane was 77 cm^2 in the cell. During the experiments, the active layer of the FO membrane faced the cycle of feed solution, while the porous supporting layer was subjected to the draw solution. The co-current cross-flow mode was used in the experiment, and there were no mesh spacers placed in the channel. Variable-speed peristaltic pumps (WT600-2J, Longerpump, Baoding) were used to control the flow velocities of both the feed and the draw solutions. The rotating speed was set at 100 rpm, and the flow velocity was approximately 3.28 mL/s, which was equal to a cross-sectional velocity of 3.03 cm/s on both sides. The feed solution tank was installed on a digital scale (UW6200H, Shimadzu, Japan) to determine the weight change to calculate the water flux through the membrane. The temperature was measured by a digital conductivity meter (Multi 3430, Tetracon 925, WTW, Germany) in the draw solution tank to monitor the salt reverse transport through the FO membrane. The data from the
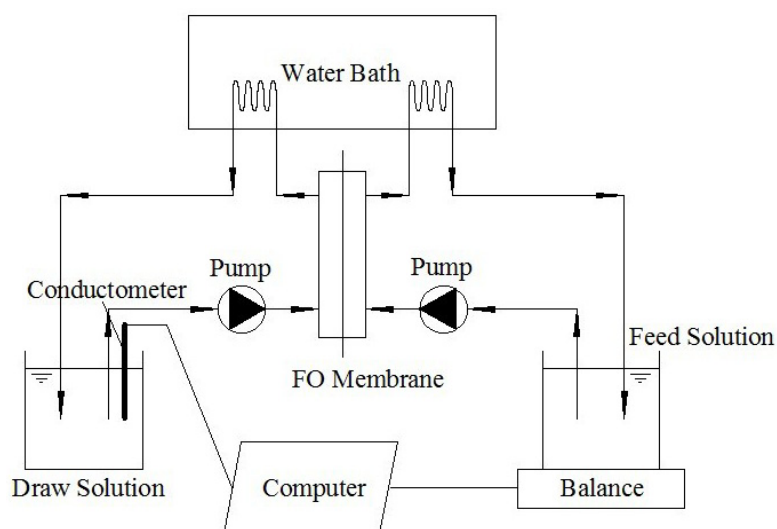

Fig. 1 Schematic diagram of the bench-scale forward osmosis (FO) system for the membrane fouling test

digital conductivity meter and the digital scale were recorded using a computer at the predetermined time intervals. The temperature and the pH were important factors that influenced the flux and the removal efficiency (You *et al.* 2012, Xie *et al.* 2012). To keep the temperature and the pH consistent during the experiments, the feed solution was adjusted to pH 7 by adding hydrochloric acid and sodium hydroxide while the temperature of the solution was kept at 30 ± 1°C by soaking part of the pipeline into water bath (DKB-1915, Jinghong, Shanghai).

The initial draw solution used in all experiments was 2 mol/L NaCl with a volume of 1.5 L. The feed solution was 2 L of deionized-water diluted standard organic solution; the addition of 10 mM NaCl was used as the background electrolytes in the feed solution. The control experiment was performed with deionized water as a feed solution. Before the experiments, deionized water was used in both the draw and the feed solutions to rinse the FO membrane at the same cross-flow velocity. Next, the membrane coupon was stabilized for 30 min for each experiment. All of the tests were performed for 5 h.

2.4 Analytical methods

The total organic carbon (TOC) of the standard organic solutions was measured using a TOC analyzer (TOC-L CPH, Shimadzu, Japan). The temperature and conductivity of the draw solution was monitored using an electric conductivity meter (Multi 3430, Tetracon 925, WTW, Germany). The weight change of the feed solution was measured using a digital balance (UW6200H, Shimadzu, Japan).

The fouled membranes were dried in air for 24 h, followed by drying in an oven for half an hour. A small piece (3×2 cm^2) of fouled membrane was cut into pieces in 15 mL of ultrapure water, and then oscillated in an oscillator for 10 min. The membrane surface before and after the experiment was characterized using a Fourier transform infra-red spectrometer (Nicolet iS5, Thermo, US) equipped with an attenuated total reflection (ATR) accessory. The used membranes were also examined using a Scanning Electron Microscope (XL30, Philips, Netherlands).

3. Results and discussion

3.1 Effect of different organics on the membrane flux

Organic fouling is known to have a significant influence on membrane processes. Organic fouling will lead to the formation of a cake-layer, thus reducing the efficiency of membrane filtration systems (Mi and Elimelech 2010). For SA, BSA and TA, three initial concentrations (50, 100 and 200 mg/L) were tested. A control test in the absence of the organics was conducted to distinguish the effect of membrane fouling and dilution in DS. All of the results were normalized by the initial water flux determined in the control test (8.42 L•m^{-2}•h^{-1}).

Fig. 2(a) presents the effect of SA at different concentrations on the permeate flux of the FO membrane. SA in the FS resulted in a noticeable permeate flux decline for the FO membrane. This fouling became more severe at a high SA concentration: the flux decreased by approximately 18% to 6.84 L•m^{-2}•h^{-1} after 5 h of operation at the SA concentration of 200 mg/L. Compared with the SA of 200 mg/L, SA at lower concentrations exhibited a slight fouling tendency, which demonstrates that the fouling extent was related to the SA concentration -- higher SA concentration led to increased SA deposition on the membrane and more severe fouling. Figs. 2(b) and (c) show that
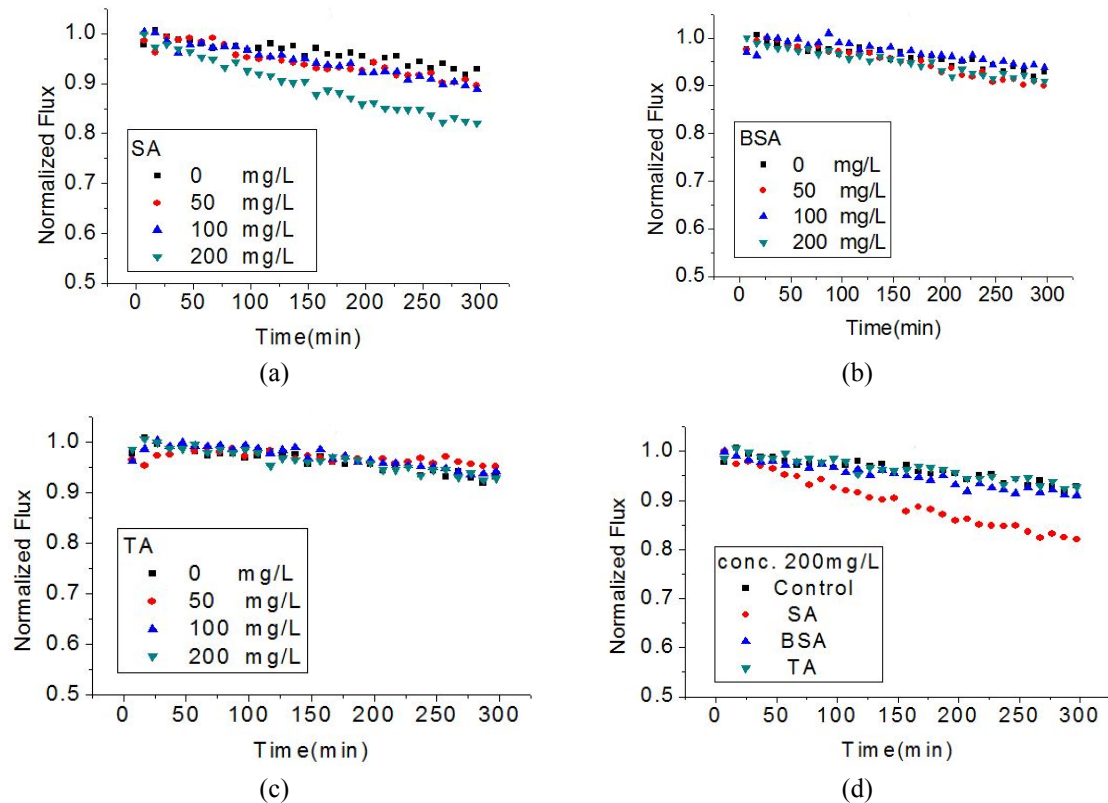
Fig. 2 Water flux decline of the FO processes: (a) flux curves of SA; (b) flux curves of BSA; (c) flux curves of TA; (d) flux curves of 200 mg/L of organics

the increase of BSA and TA concentrations resulted in no significant difference on their fouling potential for the FO membrane. The flux in presence of these two organic species declined relatively slowly, with less than 10% decline being observed in each test, which is comparable to the flux decline in the control test conducted with pure water as FS. Fig. 2(d) shows the permeate flux decline in the presence of 200 mg L^{-1} of the three individual organics compared with the control test. It is obvious that the flux decreased most significantly in the presence of SA. TA led to the least fouling, as its flux was almost the same as that of the control test. BSA exhibited moderate fouling potential on the membrane compared with SA and TA.

3.2 Adsorption of the organics on the membrane

The adsorption of organics onto the membrane leads to fouling in the FO process. To study the relationship between the adsorption and the fouling extent, the fouled membranes were oscillated in deionized water, and then the foulants that were detached from the membranes were characterized.

Table 1 presents the TOC concentrations after desorption of all membranes. The TOC desorbed from the membrane in the control test was 1.47 mg/L, which was equivalent to 0.037 mg-TOC/cm^2. This TOC can be attributed the dissolution of organics from the membrane itself. The result

Table 1 Characteristics of the fouled FO membrane

	Concentration [a] (mg/L)	TOC [b] (mg/L)	Contact Angle [c] (°)	Adsorption [d] (mg.cm^{-2})
Control	0	1.47	88.9	0.0037
SA	50	13.72	76.0	0.0343
SA	100	30.16	80.4	0.0754
SA	200	146.8	95.2	0.3670
SA[e]	200	2.56	67.6	0.0064
BSA	50	1.33	98.7	0.0033
BSA	100	1.90	104.4	0.0047
BSA	200	2.00	107.8	0.0050
TA	50	1.23	86.9	0.0031
TA	100	1.35	90.3	0.0034
TA	200	1.15	80.2	0.0029

Notes:
[a] The concentration of the organics in the feed solution
[b] The Total Organic Carbon (TOC) after desorption
[c] The Contact Angle of the fouled membrane
[d] The average adsorption amount of organics on the FO membrane
[e] The cake-layer on fouled membrane was peeled off

indicates that significant amount of SA was adsorbed onto the membrane. The adsorbed amount increased from 0.0343 to 0.367 mg/cm^2 as the SA concentration in the feed solution increased from 50 to 200 mg/L. The increased SA adsorption is consistent with the decline of the permeate flux. In addition, an obvious cake-layer was observed on the SA-fouled membranes, which will be further discussed in section 3.3.2. The cake-layer of the membrane fouled by 200 mg/L SA was easily peeled off by hand, and after the cake-layer was peeled off from the membrane, the membrane was oscillated in deionized water again to desorb the remaining foulant on the membrane. The TOC dissolved from the membrane decreased from 0.367 to 0.0064 mg/cm^2, which proved that the cake-layer caused by fouling is one of the dominant factors that affect the flux.

The adsorption of BSA and TA was negligible compared with SA. The amounts of TA adsorbed onto the membrane at the three concentrations were all approximately 0.003 mg/cm^2. The adsorption amounts of BSA at the three concentrations were also close to each other, i.e., 0.0033, 0.0047 and 0.005 mg/cm^2. The results are consistent with the fouling potentials of the three organics, as shown in Section 3.1. Previous studies (Mi and Elimelech 2008) indicated that foulant–foulant interaction plays an important role in determining the rate and extent of organic fouling and the intermolecular adhesion force of BSA is reported to be poorer than that of SA. Thus, compared to SA, slighter fouling would be formed on the membrane when BSA was used as the model foulant, which accorded with the results in this study. With stronger intermolecular adhesion forces, hydrodynamic conditions for favorable foulant deposition leading to cake formation are more readily attained (Mi and Elimelech 2008). The obvious cake-layer on membrane fouled by SA also indicated that SA foulant has the strongest foulant–foulant

interaction.

The contact angle of the fouled membranes is also presented in Table 1. The contact angle of the fouled membrane increased from 76.0° to 95.2° as the concentration of SA in the feed solution increased from 50 to 200 mg/L. In contrast, those values of BSA- and TA-fouled membranes only slightly changed with the original concentrations of the two organics in the FS. The variation tendency of the contact angle was also consistent with the flux behaviour. The adsorption of SA increased the contact angle and the hydrophobic nature of the fouled membrane.

3.3 Characterization of fouled membranes

3.3.1 FTIR analysis

FTIR is an effective protocol to characterize the chemical composition of the FO membrane (Alsvik and Hagg 2013). Different groups on the membrane surface have their own characteristic absorption peaks on the infrared spectrum. All membranes used in this study were characterized using FTIR. The virgin membrane exhibited several FTIR peaks (Fig. 3). The bands at 1743 cm^{-1}, 1231 cm^{-1}, 1046 cm^{-1}, and approximately 1370 cm^{-1} are assigned to the vibration of the –C=O group, the –C–O–C– bond, the –C–O–C bond in the pyranose ring, and the –CH$_3$ bond, respectively. All of them were characteristic bands of cellulose triacetate (Nguyen *et al.* 2013), the bases of the FO membrane.

After SA fouling, the FTIR spectra of membrane changed significantly. Moreover, there were great differences between the membranes fouled at different SA concentrations. For the membrane fouled by 50 mg/L SA, the intensities of the characteristic bands of the virgin membrane declined significantly. When the membrane was fouled by SA solution of 100 mg/L and 200 mg/L, the bands at 1743 cm^{-1} and 1231 cm^{-1} almost disappeared. It is obvious that the adsorption of SA reduced the FTIR-responses of the original groups on the membrane surface. In addition, new bands appeared at 1412 cm^{-1} and 1601 cm^{-1}, which can be attributed to –COO– in the carboxylate groups. These bands increased as the SA concentration in the FS was increased from 50 mg/L to 100 mg/L. Their increase became insignificant as the SA concentration in the feed solution was further increased over 100 mg/L. This result indicates that the SA exerted a strong fouling for the membrane, and the thickness of the cake-layer increased with the initial SA concentration in the FS.
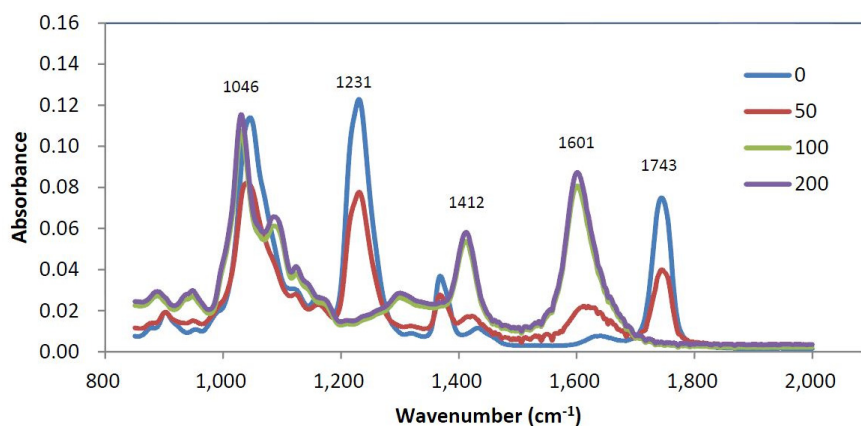

Fig. 3 FTIR spectra of membranes fouled by SA of concentrations of 0, 50, 100 and 200 mg/L
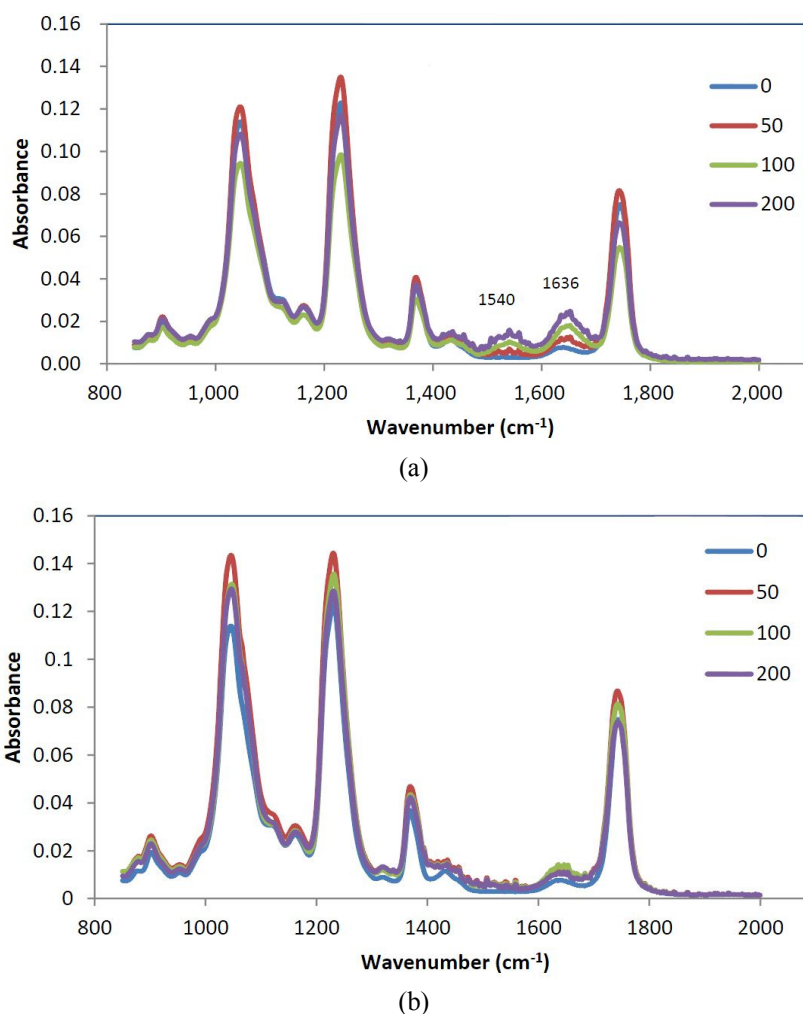
(a)

(b)

Fig. 4 FTIR images of membranes fouled by (a) BSA; and (b) TA. The concentrations of the organics in feed solutions were 0, 50, 100 and 200 mg/L

Figs. 4(a) and (b) show the FTIR spectra of BSA and TA fouled membrane, respectively. The IR spectra of TA fouled membrane were nearly the same as that of the virgin one, except for slight changes in band intensities. These results are consistent with the negligible TA fouling on the membrane observed in the filtration test. The BSA fouled membrane exhibited symbolic protein bands at 1540 cm^{-1} and 1636 cm^{-1}; however, their intensities were quite low, and negligibly changed with different BSA concentrations in the FS. This trend is consistent with the TOC amount desorbed from the BSA fouled membranes, indicating that only a small amount of BSA deposited onto the membrane surface and caused slight fouling for the membrane.

3.3.2 SEM characterization

The morphology and the structure of the fouled FO membranes were characterized using scanning electron microscopy (SEM). Fig. 5 shows SEM images of the active layers of the fouled

FO membranes. A close scrutiny of the SEM images of the fouled membranes can assist in revealing the formation of organic or inorganic fouling on the membrane surface. Organic foulants generally possess irregular and random structures, as depicted in Figs. 5(c) and (e), while surface salt foulants have well-defined crystalline structures. Few organic foulants were observed on the surfaces of the BSA- and TA- fouled membranes, as shown in Figs. 5(e) and (g). In particular, for the TA-fouled membrane, most of the surface was occupied by salts. However, the SA-fouled membrane exhibited more significant foulant accumulation on the surface compared with the membranes fouled by BSA and TA, as shown in Fig. 5(c). A gel-like layer was observed on the SA-fouled membrane. A previous study suggested that the alginate gel layer could be formed in the fouling experiment, which was composed of cross-linking long chain molecules forming a relatively thick network structure (Mi and Elimelech 2010). The severe fouling of SA fits well with the significant membrane flux decline, as described in Section 3.1.
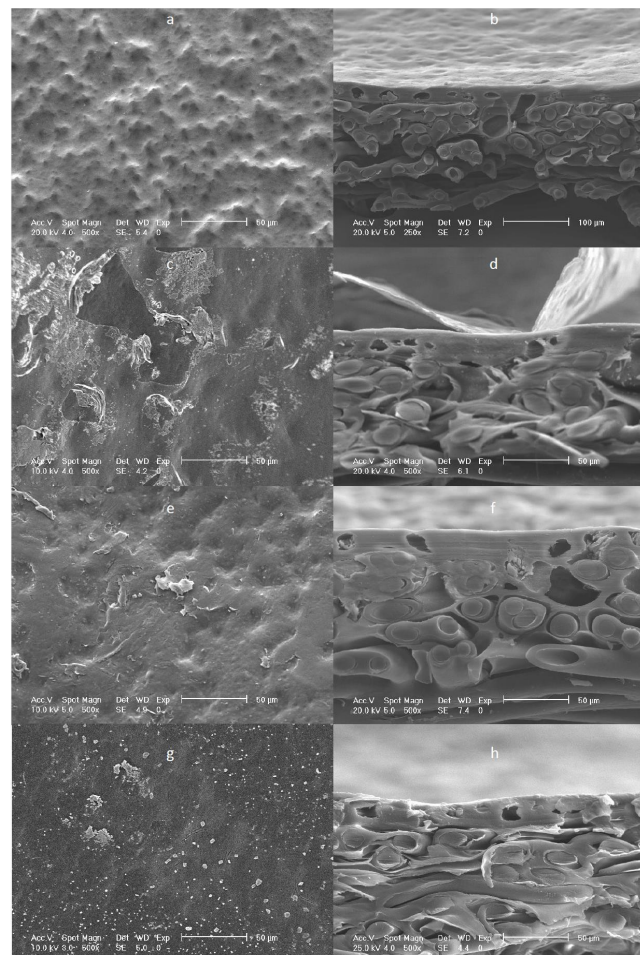

Fig. 5 SEM micrographs of FO membranes. Figs. 5(a), (c), (e) and (g) are surface micrographs of the virgin membrane, the membrane fouled by SA, the membrane fouled by BSA and the membrane fouled by TA, respectively. Figs. 5(b), (d), (f) and (h) are cross-sectional micrographs of these membranes shown in Figs. 5(a), (c) (e) and (g), respectively

To better understand the role that the organics played on the membrane fouling, the SEM images of the cross-sections of the fouled membranes were also analyzed. The cross-sectional SEM images show clearly the asymmetric structure. The cross-sectional images of the membranes fouled by BSA and TA (Figs. 5(d) and (f)), were the same as that of the virgin one. There was almost no deposition of the two organics onto the surface of the membrane. In contrast, the deposition of SA was significant. A cake-layer could be clearly observed on the surface of SA-fouled membrane. To investigate the influence of organic concentration on the FS fouling, cross-sectional SEM images for two membranes fouled by different levels of FS were also taken. The thickness of the cake-layer was measured. The membrane fouled with 50 mg/L SA had a thickness of 0.7 μm; as the concentration was increased to 200 mg/L, the thickness reached approximately to 3 μm. These observations imply that the fouling extent is related to the composition in the FS, which agrees well with the observation regarding the declining patterns of the permeate water flux in the presence of the organics. Overall, the implication here is that the type and the concentration of the foulant exerts a significant influence on the FO membrane fouling process.

4. Conclusions

In this study, three different organic species were used to investigate their influence on the fouling of a forward osmosis membrane. The membrane fouling caused by the organic species reduced the permeate flux, especially in the presence of 200 mg/L of SA (the average flux declined from 8.42 to 6.84 L•m^{-2}•h^{-1}). This reduction is caused by the SA adsorption onto the membrane, which formed a cake-layer and subsequently enhanced ion concentration polarization and osmotic pressure within the cake layer near the membrane surface. According to a previous study, the severe fouling caused by SA was possibly due to the intermolecular adhesion force, which played an important role in determining the rate and extent of organic fouling. With the strongest intermolecular interactions, alginate formed a cake layer under all tested hydrodynamic conditions. FTIR analysis and SEM images demonstrated the adsorption of organic materials from the feed solution as well as the significant changes in the functional groups and the cake-layer on the membrane surface. In addition, the fouling caused by BSA and TA only slightly affected the permeate flux, which were consistent with their insignificant effect on the FTIR spectra and the SEM images of the membranes. The TOC desorbed from the fouled membranes (i.e., significant TOC desorption from the SA-fouled membrane vs. insignificant TOC desorption from the BSA- and TA-fouled membranes) also confirmed the fouling potentials of the three organic materials on the membrane. The results proved that the adsorption of organic materials influenced the FO membrane performance.

Acknowledgments

References

Alsvik, I.L. and Hagg, M.B. (2013), "Preparation of thin film composite membranes with polyamide film on hydrophilic supports", *J. Membr. Sci.*, **428**, 225-231.

Bennett, A. (2005), "Membranes in industry: Facilitating reuse of wastewater", *Filtr. Sep.*, **42**(8), 28-30.

Cath, T.Y., Childress, A.E. and Elimelech, M. (2006), "Forward osmosis: Principles, applications, and recent developments", *J. Membr. Sci.*, **281**(1-2), 70-87.

Chou, S.R., Wang, R., Shi, L., She, Q.H., Tang, C.Y. and Fane, A.G. (2012), "Thin-film composite hollow fiber membranes for pressure retarded osmosis (PRO) process with high power density", *J. Membr. Sci.*, **389**, 25-33.

Cornelissen, E.R., Harmsen, D., Ruiken, C.J. and Qin, J.J. (2008), "Membrane fouling and process performance of forward osmosis membranes on activated sludge", *J. Membr. Sci.*, **319**(1-2), 158-168.

Dalton, S.K., Brant, J.A. and Wiesner, M.R. (2005), "Chemical interactions between dissolved organic matter and low-molecular weight organic compounds: impacts on membrane separation", *J. Membr. Sci.*, **266**(1-2), 30–39.

Grant, G.T., Morris, E.R., Rees, D.A., Smith, J.C. and Thom, D. (1973), "Biological interaction between polysaccharides and divalent cations: the egg-box model", *FEBS Lett.*, **32**, 195-198.

Gu, Y.S., Wang, Y.N., Wei, J. and Tang, C.Y.Y. (2013), "Organic fouling of thin-film composite polyamide and cellulose triacetate forward osmosis membranes by oppositely charged macromolecules", Water Res., **47**(5), 1867-1874.

Guo, W., Ngo, H.H. and Li, J.A. (2012), "mini-review on membrane fouling", *Bioresour. Technol.*, **122**, 27-34.

Holloway, R.W., Childress, A.E., Dennett, K.E. and Cath, T.Y. (2007), "Forward osmosis for concentration of anaerobic digester centrate", Water Res., Sep, **41**(17), 4005-4014.

Lay, W.C.L., Zhang, Q.Y., Zhang, J.S., McDougald, D., Tang, C.Y. and Liu, Y. (2011), "Study of integration of forward osmosis and process: Membrane performance under elevated salt environment" Desalination, **283**, 123-130.

Lee, S., Boo, C., Elimelech, M. and Hong, S. (2010), "Comparison of fouling behavior in forward osmosis (FO) and reverse osmosis (RO)", *J. Membr. Sci.*, **365**(1-2), 34-39.

Linares, R.V., Yangali-Quintanilla, V., Li, Z. and Amy, G. (2012), "NOM and TEP fouling of a forward osmosis (FO) membrane: Foulant identification and cleaning", *J. Membr. Sci.*, **421**, 217-224.

Lin, Y.L., Chiang, P.C. and Chang, E.E. (2007), "Removal of small trihalomethane precursors from aqueous solution by nanofiltration", *J. Hazard. Mater.* **146**(1-2), 20-29.

Ma, H.Z., Allen, H.E. and Yin,Y.J. (2001), "Characterization of isolated fractions of dissolved organic matter from natural waters and a wastewater effluent", *Water Res.*, **35**(4), 985-996.

McCutcheon, J.R., McGinnis, R.L. and Elimelech, M. (2006), "Desalination by ammonia-carbon dioxide forward osmosis: Influence of draw and feed solution concentrations on process performance", J. Membr. Sci., **278**(1-2), 114-123.

Mi, B. and Elimelech, M. (2008), "Chemical and physical aspects of organic fouling of forward osmosis membranes", *J. Membr. Sci.*, **320**(1-2), 292-302.

Mi, B. and Elimelech, M. (2010), "Organic fouling of forward osmosis membranes: Fouling reversibility and cleaning without chemical reagents", *J. Membr. Sci.*, **348**(1-2), 337-345.

Mylon, S.E., Chen, K.L. and Elimelech, M. (2004), "Influence of natural organic matter and ionic composition on the kinetics and structure of hematite colloid aggregation: Implications to iron depletion in estuaries", *Langmuir*, **20**(21), 9000- 9006.

Nguyen, A., Azari, S. and Zou, L.D. (2013), "Coating zwitterionic amino acid L-DOPA to increase fouling resistance of forward osmosis membrane", *Desalination*, **312**, 82-87.

Phuntsho, S., Vigneswaran, S., Kandasamy, J., Hong, S., Lee, S. and Shon, H.K. (2012), "Influence of temperature and temperature difference in the performance of forward osmosis desalination process", *J. Membr. Sci.*, **415**, 734-744.

Shaffer, D.L., Yip, N.Y., Gilron, J. and Elimelech, M. (2012), "Seawater desalination for agriculture by integrated forward and reverse osmosis: Improved product water quality for potentially less energy", *J. Membr. Sci.*, **415**, 1-8.

She, Q.H., Jin, X. and Tang, C.Y.Y. (2012), "Osmotic power production from salinity gradient resource by pressure retarded osmosis: Effects of operating conditions and reverse solute diffusion", *J. Membr. Sci.*, **401**, 262-273.

She, Q.H., Wong, Y.K.W., Zhao, S.F. and Tang, C.Y.Y. (2013), "Organic fouling in pressure retarded osmosis: Experiments, mechanisms and implications", *J. Membr. Sci.*, **428**, 181-189.

Tang, C.Y., She, Q., Lay, W.C.L., Wang, R. and Fane, A.G. (2010), "Coupled effects of internal concentration polarization and fouling on flux behavior of forward osmosis membranes during humic acid filtration", *J. Membr. Sci.*, **354**(1-2), 123-133.

Tang, C.Y.Y., Chong, T.H. and Fane, A.G. (2011), "Colloidal interactions and fouling of NF and RO membranes: A review. Advances in Colloid and Interface Science" May", **164**(1-2), 126-143.

Wei, J., Qiu, C., Tang, C.Y., Wang, R. and Fane, A.G. (2011), "Synthesis and characterization of flat-sheet thin film composite forward osmosis membranes", *J. Membr. Sci.*, **372**(1-2), 292-302.

Xie, M., Price, W.E. and Nghiem, L.D. (2012), "Rejection of pharmaceutically active compounds by forward osmosis: Role of solution pH and membrane orientation", *Sep. Purif. Technol.*, **93**, 107-114.

You, S.J., Wang, X.H., Zhong, M., Zhong, Y.J., Yu, C. and Ren, N.Q. (2012), "Temperature as a factor affecting transmembrane water flux in forward osmosis: Steady-state modeling and experimental validation", *Chem. Eng. J.*, **198**, 52-60.

Zhang, J., Loong, W.L.C., Chou, S., Tang, C., Wang, R. and Fane, A.G. (2012), "Membrane biofouling and scaling in forward osmosis membrane bioreactor", *J. Membr. Sci.*, **403**, 8-14.

Zhao, S., Zou, L., Tang, C.Y. and Mulcahy, D. (2012), "Recent developments in forward osmosis: Opportunities and challenges", *J. Membr. Sci.*, **396**, 1-21.

CC